

## **Inhibition Effects and Theoretical Studies of Synthesized Novel Bisaminothiazole Derivatives as Corrosion Inhibitors for Carbon Steel in Sulphuric Acid Solutions**

*M. Abdallah<sup>1,2,\*</sup>, A.M. El Defrawy<sup>1,3</sup>, I. A. Zaaferany<sup>1</sup>, M. Sobhi<sup>2,5</sup>, A.H.M. Elwahy<sup>4</sup>, and M. R. Shaaban<sup>1,4</sup>*

<sup>1</sup>Chem. Dept, Fac. of Appl. Science, Umm Al-Qura University, Makkah Al-Mukarramah, Saudi Arabia.

<sup>2</sup>Chem. Dept, Fac. of Science, Benha University, Benha, Egypt

<sup>3</sup>Chem. Dept, Fac. of Science, Mansoura University, Mansoura, Egypt.

<sup>4</sup>Chem. Dept, Fac. of Science, Cairo University, Giza, Egypt.

<sup>5</sup>Chem. Dept, Fac. of Science, Tabuk University, Tabuk, Saudi Arabia.

\*E-mail: [metwally555@yahoo.com](mailto:metwally555@yahoo.com)

*Received:* 8 December 2013 / *Accepted:* 3 February 2013 / *Published:* 2 March 2014

---

The inhibition effect of four synthesized novel bis(aminothiazole) derivatives on the corrosion of carbon steel in 0.5M H<sub>2</sub>SO<sub>4</sub> solution was investigated using galvanostatic, potentiodynamic anodic polarization and weight loss techniques. The inhibitive effect was ascribed to the formation of insoluble complex adsorbed on the steel surface and the adsorption process follows Langmuir adsorption isotherm. A theoretical study of the corrosion inhibition efficiency of these bis(aminothiazole) derivatives, was carried out using density functional theory (DFT) at the B3LYP/6-31G(d) level of theory. Molecular properties related to the inhibition efficiency of these inhibitors were obtained and found in good correlation with the inhibition efficiency obtained from different techniques.

---

**Keywords:** Carbon steel, Bisaminothiazole Derivatives, DFT studies, weight loss, acid inhibition

### **1. INTRODUCTION**

Carbon steel is widely applied as the constructional materials in many industries e.g. petroleum pipes lines due to its excellent mechanical properties and low cost. The other important fields of application are acid pickling, industrial cleaning, acid descaling, oil recovery and the petrochemical process [1]. Sulphuric acid is one of the chemicals most widely used for the removal of undesirable scale and rust in many industrial processes. Due to the exposure of carbon steel to corrosive acidic solutions, it is susceptible to corrosion. The use of corrosion inhibitors to prevent metal dissolution is

therefore essential. Generally, corrosion inhibitors are organic compounds containing heteroatoms such as nitrogen, oxygen or sulphur in their chemical structure [2-12]. Organic compounds bearing heteroatoms with high electron density such as phosphor, sulphur, nitrogen, oxygen or those containing multiple bonds which are considered as adsorption centers, are effective as corrosion inhibitor [7-10]. The compounds contain both nitrogen and sulphur in their molecular structure has exhibited greater inhibition compared with those contain only one of these atoms [11-12]. In literature many thiazole derivatives have been studied as corrosion inhibitors and found that thiazole derivatives have good corrosion inhibition effect [13-14]. The inhibition property of thiazole compounds is attributed to their molecular structure. The planarity and pairs of free electrons in heteroatoms are important characteristics that determine the adsorption of these molecules on the metal surface. Thiazole derivatives are considered as non-cytotoxic substances. This environmentally friendly property makes them favorable to be used in practice, replacing some toxic organic inhibitors in agreement with the new environmental restrictions need to use green ones [15-16]. On the other hand, the inhibiting efficiency of organic compounds is strongly dependent on the structure and chemical properties of the layer adsorbed on the metal surface. The strength of adsorbed layer is related to the functional groups connected to aromatic ring [17]. The adsorption of organic compounds depends mainly on the electronic structure of the molecule and that the inhibition efficiency increases with the increase in the number of aromatic ring [18]. In this context, theoretical chemistry has been used recently to explain the mechanism of corrosion inhibition, such as quantum chemical calculations, which have been proved to be a very powerful tool for studying the mechanism [19-21]. The reactive ability of the inhibitor is closely linked to their frontier molecular orbitals (MO), including highest occupied molecular orbital, HOMO, and lowest unoccupied molecular orbital, LUMO, and the other parameters such as hardness and softness. The present study aimed to investigate the inhibition effect of the synthesized novel bis-aminothiazole compounds on the corrosion of C-steel in 0.5 M H<sub>2</sub>SO<sub>4</sub> solution using galvanostatic polarization, potentiodynamic anodic polarization and weight loss techniques. Density functional theory used to calculate some quantum chemical parameters which will assist in the interpretation of inhibition process.

## 2. EXPERIMENTAL TECHNIQUES

### 2.1. Synthesis of bis(aminothiazoles).

#### *General procedure:*

A mixture of appropriate bis( $\alpha$ -bromoacetophenones) derivative (20 mmol), thiourea or N-methylthiourea (20 mmol), and least amount of *i*-PrOH were mixed in a process vial. The vial was capped properly and irradiated by microwaves using pressurized conditions (249 psi, 120 °C) for 20-30 min. The vial contents were taken in ether, collected by filtration, washed with EtOH, dried, and finally recrystallized from EtOH/dioxane to afford the corresponding bis(thiazoles) **2a-d** in excellent yield. The physical and spectral data of the synthesized compounds are listed below.

**4,4'-(4,4'-(ethane-1,2-diylbis(oxy))bis(4,1-phenylene))dithiazol-2-amine (6) (*p*-Bis-AT):** mp. 301 °C; ir: (potassium bromide) 3389, 3281 (NH<sub>2</sub>), 1608 (C=N) cm<sup>-1</sup>; <sup>1</sup>H nmr: δ 3.37 (br, 4H), 4.37 (s, 4H), 7.03 (s, 2H), 7.05 (d, 4H, *J* = 9 Hz), 7.77 (d, 4H, *J* = 9 Hz). ms: *m/z* (%) 412 (M<sup>+</sup>, 13). *Anal.* Calcd. for C<sub>20</sub>H<sub>18</sub>N<sub>4</sub>O<sub>2</sub>S<sub>2</sub>: C, 58.52; H, 4.42; N, 13.65. Found: C, 58.56; H, 4.40; N, 13.68%.

**4,4'-(4,4'-(ethane-1,2-diylbis(oxy))bis(4,1-phenylene))bis(N-methylthiazol-2-amine) (7) (*p*-Bis-MAT):** mp. 294 °C; ir: (potassium bromide) 3485(NH), 1608 (C=N) cm<sup>-1</sup>; <sup>1</sup>H nmr: δ 2.87 (s, 6H), 3.72 (br, 4H), 4.46 (s, 4H), 7.05 (s, 2H), 7.06 (d, 4H, *J* = 9 Hz), 7.76 (d, 4H, *J* = 9 Hz). ms: *m/z* (%) 438 (M<sup>+</sup>, 38). *Anal.* Calcd. for C<sub>22</sub>H<sub>22</sub>N<sub>4</sub>O<sub>2</sub>S<sub>2</sub>: C, 60.25; H, 5.06; N, 12.78. Found: C, 60.22; H, 5.04; N, 12.80%.

**4,4'-(2,2'-(ethane-1,2-diylbis(oxy))bis(2,1-phenylene))dithiazol-2-amine (8) (*o*-Bis-AT):** mp. 269 °C; ir: (potassium bromide) 3488, 3465(NH<sub>2</sub>), 1608 (C=N) cm<sup>-1</sup>; <sup>1</sup>H nmr: δ 3.77 (br, 4H), 4.44 (s, 4H), 7.04 (s, 2H), 7.08 (t, 2H, *J* = 9 Hz), 7.26 (d, 2H, *J* = 9 Hz), 7.36 (t, 2H, *J* = 9 Hz), 7.67 (d, 2H, *J* = 9 Hz). ms: *m/z* (%) 412 (M<sup>+</sup>, 12). *Anal.* Calcd. for C<sub>20</sub>H<sub>18</sub>N<sub>4</sub>O<sub>2</sub>S<sub>2</sub>: C, 58.52; H, 4.42; N, 13.65. Found: C, 58.49; H, 4.44; N, 13.62%.

**4,4'-(2,2'-(ethane-1,2-diylbis(oxy))bis(2,1-phenylene))bis(N-methylthiazol-2-amine) (9) (*o*-Bis-MAT):** mp. 289 °C; ir: (potassium bromide) 3485(NH), 1608 (C=N) cm<sup>-1</sup>; <sup>1</sup>H nmr: δ 2.91 (s, 6H), 3.72 (br, 4H), 4.51 (s, 4H), 7.05 (s, 2H), 7.06 (t, 2H, *J* = 9 Hz), 7.23 (d, 2H, *J* = 9 Hz), 7.44 (t, 2H, *J* = 9 Hz), 7.70 (d, 2H, *J* = 9 Hz). ms: *m/z* (%) 438 (M<sup>+</sup>, 34). *Anal.* Calcd. for C<sub>22</sub>H<sub>22</sub>N<sub>4</sub>O<sub>2</sub>S<sub>2</sub>: C, 60.25; H, 5.06; N, 12.78. Found: C, 60.24; H, 5.07; N, 12.75%.

## 2.2. Materials

Carbon steel of type L-52 used in this study has the following chemical composition (wt %) : C 0.26 %, Mn 1.35%, S 0.04 %, Nb 0.005%, V 0.02%, Ti 0.03% and the rest is iron. The galvanostatic polarization was performed using specimens in the form of rods of 1 cm<sup>2</sup> exposed surface area as a working electrode. For weight loss tests, small rectangular coupons of the dimensions 1.0 cm x 2.0 cm x 0.3 cm were used.

The testing media were aqueous aerated 0.5 M H<sub>2</sub>SO<sub>4</sub> solutions without and with different concentrations from the compounds under study. All chemicals used in this study were of analytical grade (Aldrich chemicals) and the desired temperature of each experiment was adjusted to ± 1 °C using air thermostat. The structural formula of the investigated compounds is represented in Table 1.

## 2.3. Apparatus

The weight-loss measurements were carried out in large test tubes (20 cm × 2.5 cm diameter) suspended in a thermostated water bath. Each tube was open to air.

The galvanostatic cathodic and anodic polarization measurements were carried out using three-compartment glass cell and EG&G model 363 potentiostat/galvanostat corrosion measurement system. Platinum electrode was used as a counter electrode (separated from the cell solution by a sintered glass frit) and a saturated calomel electrode (inside a luggin's probe) as a reference electrode.

The potentiodynamic anodic polarization measurements were performed using a Wenking potentiostat, type POS 73 and the X–Y recorder, type advanced, HR 2000.

The UV–visible spectrophotometric experiments were carried out using JASCO UV–VIS 530 spectrophotometer and 10 mm matched silica cell.

## 2.4. Procedures

### 2.4.1. Galvanostatic polarization

The working electrode was polished and pre-polarized prior to recording the cathodic and anodic polarization curves at each concentration of the tested solution. All the polarized curves were obtained using the direct technique at regular intervals. The duration of potential stabilization at each current density value was between 3 and 5 min.

### 2.4.2. Potentiodynamic polarization

The working electrode is the same as that used before in galvanostatic polarization techniques; the electrode surface was polished and left for 10 min as a pre-steady state prior to scanning rate of (50 mVs<sup>-1</sup>) at each concentration on the tested solution.

### 2.4.3. Weight loss measurements

The coupons were successively abraded with SiC paper to a final finish using 1200 grade paper. Before immersion in the test solution (50 ml) the dimensions of each coupon were ascertained. They were then degreased in AR grade acetone, etched in HCl for 30 s, washed with double distilled water, followed by acetone, dried and weighted. The cleaned carbon steel coupons were weighted before and after immersion in 50 ml of the test solution for a period of time up to 8 h. The average weight loss for each of the identical experiments was taken and expressed in mg cm<sup>-2</sup>.

### 2.4.4. UV- visible Spectroscopy

Using UV–visible spectrophotometric method, some experiments were carried out on the electrolyte solution of the inhibited system before and after polarization measurements.

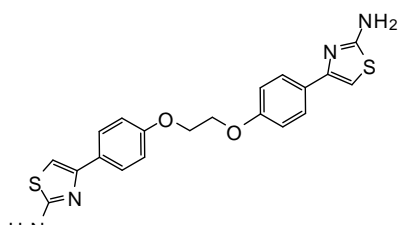
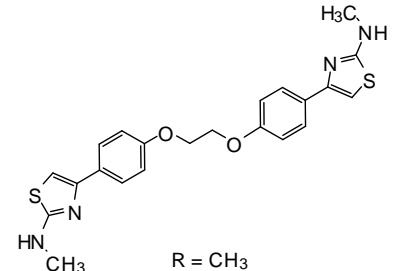
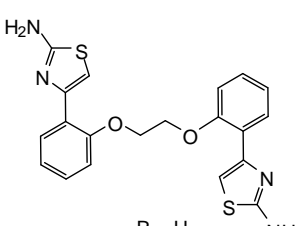
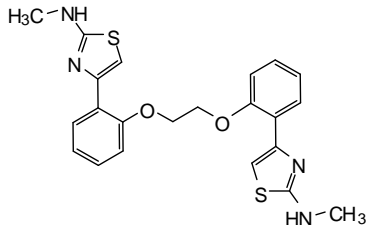
## 3. RESULTS AND DISCUSSION

### 3.1 Organic synthesis

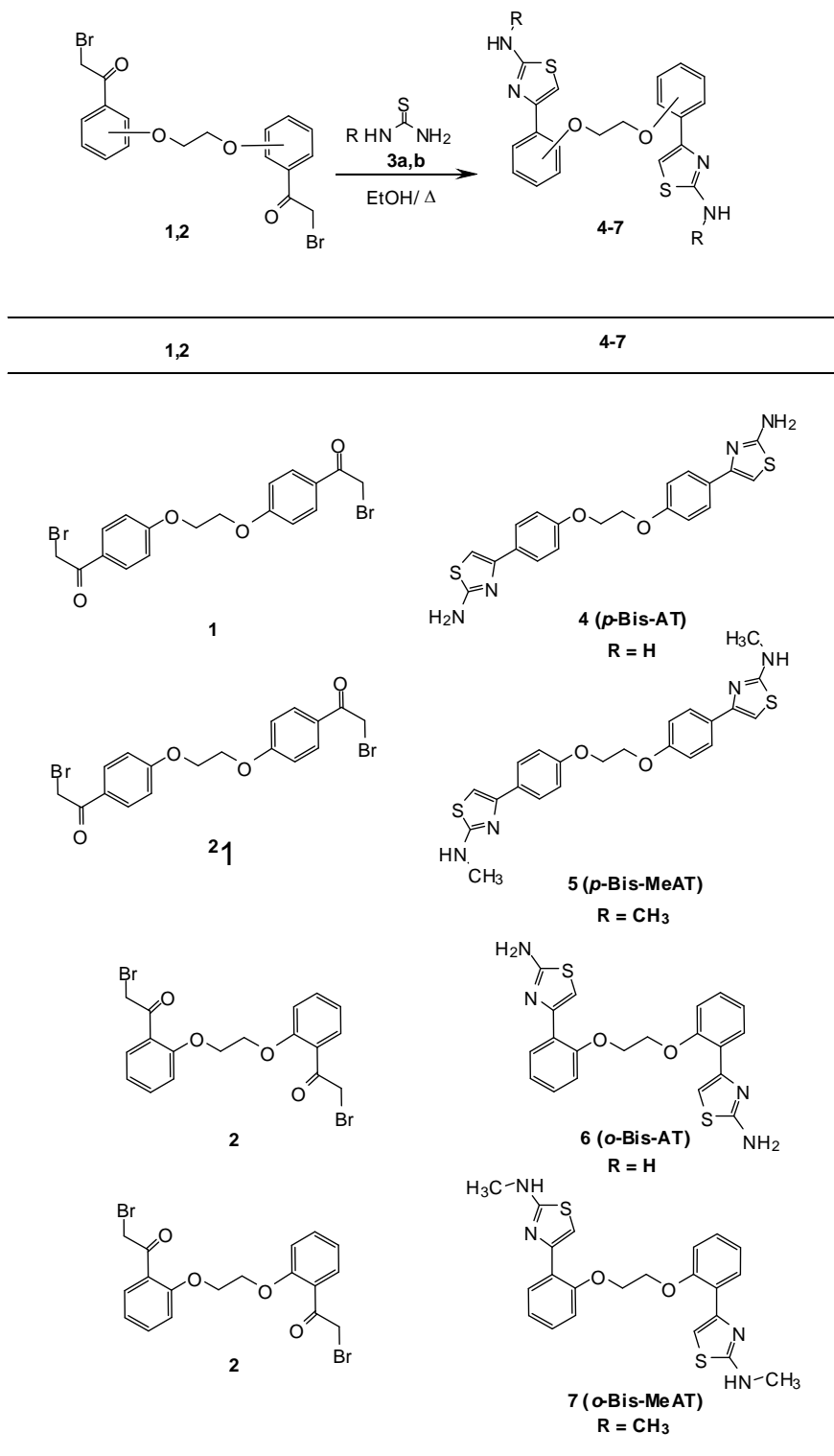
In search of an expedient methods, synthesis of the novel bis(aminothiazole) derivatives **4-7** attracted our attention. Based on the use the cyclocondensation of the versatile bis(□-

bromoacetophenones) **1** and **2** with the substituted thiourea derivatives **3a,b** under microwave irradiation as shown in scheme 1. The structures of the products **4-7** were established on the basis of their elemental analyses and spectral data (see experimental part).

**Table 1.** The chemical structures and abbreviations of the investigated bis(aminothiazole) derivatives .

Compound	Structure & Name	Chemical formula & Molecular Weight
<b>p-Bis-AT</b>	 <p style="text-align: center;">R = H</p> <p style="text-align: center;">5,5'-(4,4'-(ethane-1,2-diylbis(oxy))bis(4,1-phenylene))dithiazol-2-amine</p>	$C_{20}H_{18}N_4O_2S_2$ 410.51
<b>p-Bis-MeAT</b>	 <p style="text-align: center;">R = CH<sub>3</sub></p> <p style="text-align: center;">4,4'-(4,4'-(ethane-1,2-diylbis(oxy))bis(4,1-phenylene))bis(N-methylthiazol-2-amine)</p>	$C_{22}H_{22}N_4O_2S_2$ 438.57
<b>o-Bis-AT</b>	 <p style="text-align: center;">R = H</p> <p style="text-align: center;">5,5'-(2,2'-(ethane-1,2-diylbis(oxy))bis(2,1-phenylene))dithiazol-2-amine</p>	$C_{20}H_{18}N_4O_2S_2$ 410.51
<b>o-Bis-MeAT</b>	 <p style="text-align: center;">R = CH<sub>3</sub></p> <p style="text-align: center;">4,4'-(2,2'-(ethane-1,2-diylbis(oxy))bis(2,1-phenylene))bis(N-methylthiazol-2-amine)</p>	$C_{22}H_{22}N_4O_2S_2$ 438.57

Scheme 1



### 3.2. Galvanostatic polarization

Galvanostatic polarization curves for carbon steel in 0.5 M H<sub>2</sub>SO<sub>4</sub> at 30°C in the absence and presence of various concentrations of *o*-Bis-MeAT are shown in Fig. 1. as an example of the studied compounds. Similar curves were obtained for other compounds (not shown). Corrosion kinetic parameters, i.e., corrosion potential ( $E_{\text{corr}}$ ), cathodic and anodic Tafel slope ( $b_c$  and  $b_a$ ) and corrosion

current density ( $i_{corr}$ ), obtained by extrapolation of the Tafel lines with corrosion potential ( $E_{corr}$ ) are presented in Table 1. The inhibition efficiencies (I.E %) of the bis aminothiazole compounds in 0.5 M  $H_2SO_4$  are also given in Table 1. The percentage of the inhibition efficiency (%I.E.) was calculated using the following equation

$$I.E \% = \frac{i_{corr}^0 - i_{corr}}{i_{corr}^0} \times 100 \tag{1}$$

where,  $i_{corr}^0$  and  $i_{corr}$  are the corrosion current densities values without and with inhibitor, respectively.

From Table 1, it was shown that there is a shift in the  $E_{corr}$  values towards negative direction in the presence of various concentrations of the bis aminothiazoles compounds in 0.5 M  $H_2SO_4$ , which can be explained by a domination of the cathodic reaction inhibition [22]. However, it is clearly observed from Fig. 1 that the bis aminothiazoles compounds reduce both the anodic and cathodic current densities, indicating the inhibiting action of the compounds. In addition, from Table 1, the slopes of the anodic and cathodic Tafel lines ( $b_a$  and  $b_c$ ) were slightly changed with increasing the concentration of the tested compounds. This indicated that there was no change of the mechanism of inhibition in the presence and absence of the inhibitors. When the external current was applied, the cathode was more polarized than the anode. The higher values of Tafel slopes could be attributed to the surface kinetic process rather than the diffusion controlled process [23].

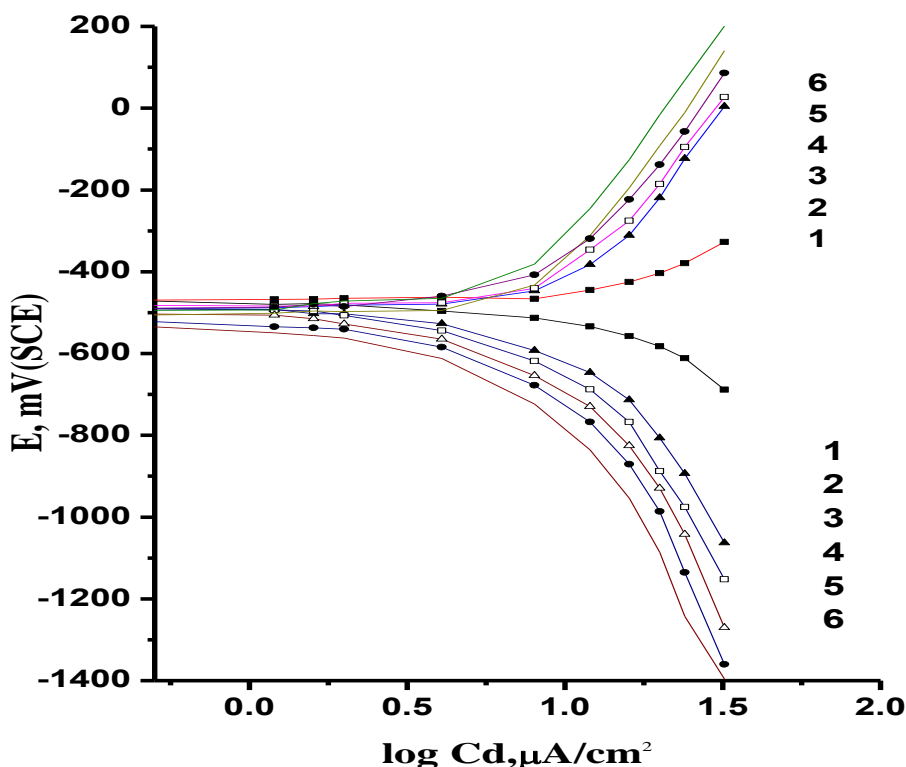
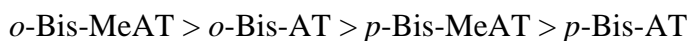


**Figure 1.** Galvanostatic polarization curves of carbon steel in 0.5M  $H_2SO_4$  containing different concentrations of compound *p*-Bis-AT (1) 0.00 (2) 100 (3) 200 (4) 300 (5) 400 (6) 500 ppm.

**Table 2.** Corrosion parameter obtained from galvanstatic polarization measurements of carbon steel in 0.5M H<sub>2</sub>SO<sub>4</sub> solution containing different concentrations of Bis aminothiazole compounds at 30 °C

Comp.	Conc., ppm	-E <sub>corr</sub> mV(SCE)	I <sub>corr</sub> mA cm <sup>-2</sup>	β <sub>c</sub> mVdec <sup>-1</sup>	β <sub>a</sub> mVdec <sup>-1</sup>	% IE
Blank	-	478	0.798	102	88	-----
<i>p</i> -Bis-AT	100	515	0.416	135	130	47.86
	200	533	0.382	150	155	52.13
	300	547	0.234	162	172	70.67
	400	550	0.192	174	177	75.93
	500	555	0.146	180	188	81.70
<i>p</i> -Bis-MeAT	100	520	0.205	146	150	74.31
	200	532	0.162	157	158	79.69
	300	537	0.128	165	169	83.95
	400	541	0.102	172	175	87.21
	500	545	0.085	176	182	89.34
<i>o</i> -Bis-AT	100	512	0.182	155	144	77.19
	200	528	0.145	162	149	81.83
	300	542	0.112	170	163	85.96
	400	553	0.072	182	174	90.98
	500	557	0.051	186	178	93.61
<i>o</i> -Bis-MeAT	100	535	0.172	158	142	78.45
	200	538	0.131	170	148	83.58
	300	542	0.106	178	152	89.40
	400	544	0.052	185	160	93.48
	500	548	0.037	190	172	95.36

The order of the inhibition efficiency of the inhibitors at different concentrations as given by polarization measurements is given as follows:



This order will be discussed later in the inhibition mechanism section.

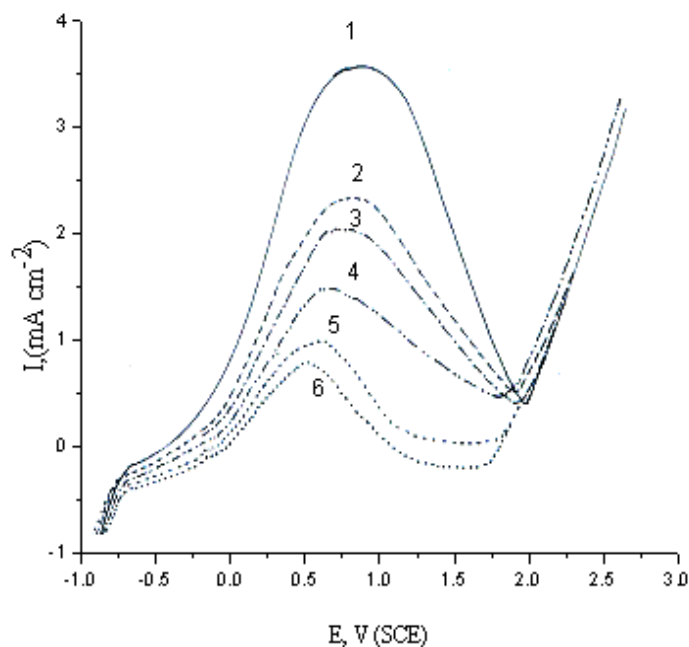
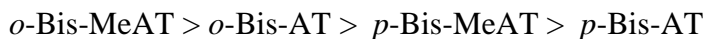
### 3.2.1. Potentiodynamic anodic polarization measurements

Fig.2 represents the effect of addition of increasing concentrations of compound (*o*-Bis-MeAT) on the potentiodynamic anodic polarization curves of carbon steel in 0.5 M H<sub>2</sub>SO<sub>4</sub> solution as an example of the studied compounds. Similar curves were obtained for other compounds (not shown). The starting potential was -1.0 V (SCE) and extended up +2.0 V at a scan rate 50 mV s<sup>-1</sup>. Inspection of the curves of Fig. 3, there is only one anodic peak noted, representing the action dissolution of Fe as Fe<sup>2+</sup>. As the concentration of the additives increases the corrosion current peak (I<sub>p</sub>) decreases and the values of peak potential E<sub>p</sub> are shifted slightly to the more positive values which suggest, the inhibiting effect of these additives.

The percentage of the inhibition efficiency (%I.E.) was calculated using the following equation:

$$\%I.E. = \left(1 - \frac{i_p^{(add)}}{i_p^{(free)}}\right) \times 100 \quad (2)$$

Where,  $i_p^{(add.)}$  and  $i_p^{(free)}$  are the peak current densities in the presence and absence of the investigated compounds. The values of  $i_p$ ,  $E_p$  and percentage inhibition (%I.E.) are listed in Table 2. It is obvious from Table 2 that the order of inhibition efficiency decreases in the following order.



**Figure 2.** Potentiodynamic anodic polarization curves of carbon steel in 0.5M H<sub>2</sub>SO<sub>4</sub> containing different Concentrations of compound *p*-Bis-AT at a scan rate of 50 mVs<sup>-1</sup>: (1)0.00ppm (2)100ppm (3)200ppm (4)300ppm (5)400ppm (6)500ppm

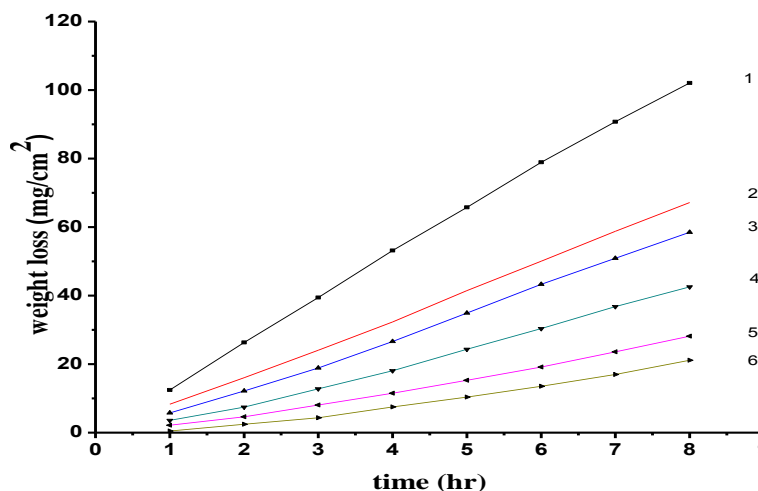
### 3.3. Weight loss measurements

Fig .3 shows the calculated weight loss (mg cm<sup>-2</sup>) for carbon steel which is exposed to 0.5 M H<sub>2</sub>SO<sub>4</sub> at 30°C in the absence and presence of different concentrations from compound *o*-Bis-MeAT, as an example of the studied compounds. Similar curves were obtained for other compounds (not shown).

The percentage of the inhibition efficiency (%I.E.) was calculated using the following equation:

$$\%IE = 1 - \frac{W_{add}}{W_{free}} \times 100 \quad (3)$$

where,  $W_{free}$  and  $W_{add}$  are the weight loss values in absence and presence of inhibitor, respectively

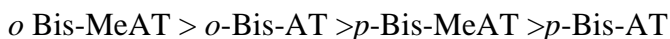


**Figure 3.** Weight loss as a function of time for carbon steel in 0.5M H<sub>2</sub>SO<sub>4</sub> solution in the absence and presence of compound I (1) 0.00ppm (2) 100ppm (3) 200ppm (4) 300ppm (5) 400ppm (6) 500ppm

**Table 3.** Corrosion parameters obtained from potentiodynamic anodic polarization measurements at scan rate 50mV/sec of carbon steel in 0.5M H<sub>2</sub>SO<sub>4</sub> solution containing different concentrations of bisamino thiazole compounds

Inhibitor system	Concentration, ppm	I <sub>p</sub> , mA cm <sup>-2</sup>	E <sub>p</sub> , V(S.C.E)	%IE	
				I <sub>p</sub>	Weight loss
Blank	0.5 M H <sub>2</sub> SO <sub>4</sub>	3.57	0.86	-----	-----
<i>p</i> -Bis-AT	100	2.35	0.83	34.00	40.88
	200	2.04	0.81	42.90	46.62
	300	1.50	0.67	58.00	69.76
	400	0.64	0.97	82.10	75.32
	500	0.54	0.79	84.90	82.46
<i>p</i> -Bis-MeAT	100	2.13	0.88	40.40	73.22
	200	1.88	0.91	47.40	78.18
	300	1.42	0.93	60.30	82.15
	400	0.58	0.97	83.75	86.83
	500	0.46	0.98	87.20	88.92
<i>o</i> -Bis-AT	100	1.98	0.87	44.60	76.12
	200	1.62	0.90	54.70	80.14
	300	1.28	0.93	64.15	84.86
	400	0.47	0.95	86.90	91.12
	500	0.31	0.98	91.40	92.98
<i>o</i> -Bis-MeAT	100	1.82	0.90	49.00	76.22
	200	1.49	0.93	58.30	81.15
	300	1.13	0.95	68.40	88.46
	400	0.33	0.98	90.80	92.66
	500	0.18	1.00	94.95	94.12

The values of percentage inhibition (%IE) obtained from weight loss method at different concentrations of the investigated inhibitors are summarized in Table 3. It has been found that the compounds under study inhibits the corrosion of carbon steel in 0.5 M H<sub>2</sub>SO<sub>4</sub> solution at all concentrations used in this study i.e. 100 – 500 ppm. It is also shown that the percentage inhibition differs at the same concentration from one compound to another and the order of inhibition decreases in the following order:



### 3.4. Adsorption isotherm

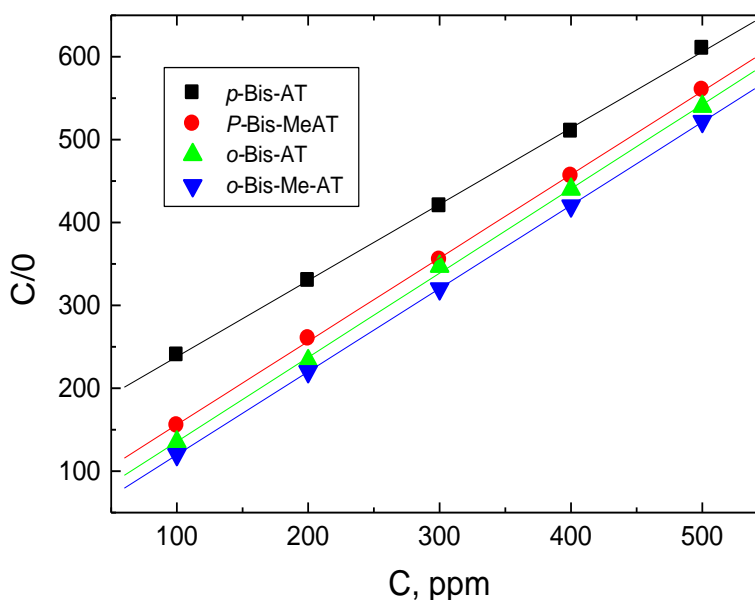
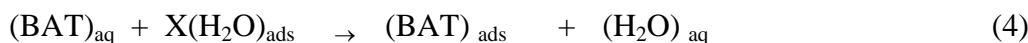


**Figure 4.** Langmuir adsorption isotherm

The inhibition of the corrosion of carbon steel in 0.5.5 M H<sub>2</sub>SO<sub>4</sub> solution by four compounds of bis aminothiazole (BAT) is based on the formation of adsorbed layer on the steel surface. The adsorption of BAT molecules is regarded as quasi substitution process between the BAT in the aqueous phase (BAT)<sub>aq</sub> and the water molecule adsorbed on the metal surface (H<sub>2</sub>O)<sub>ads</sub>



where, X is the size ratio, that is ,the number of water molecules replaced by one of BAT molecule.

It is essential to know the mode of adsorption isotherm where these experimental results represent. Attempts were made to fit the surface coverage (θ) values to various adsorption isotherm, including Langmuir, Frumkin , Freunlich and Temkin.

By far the best results were obtained fitting Langmuir adsorption isotherm. The relation between the surface coverage (θ) defined by (IE/100) and the concentration (C) can be represented by the Langmuir isotherm that is given by [24]:

$$C/\theta = 1/K + C \quad (5)$$

where K is the equilibrium constant of adsorption. Plotting C / $\theta$  versus C gave straight line with slope equal unity (Figure 4). This indicates that the adsorption of BAT molecules on the steel surface follows Langmuir adsorption isotherm. From these results one postulates that there is no interaction between the adsorbed species.

#### 4. QUANTUM CHEMICAL CALCULATIONS

Density Functional theory (DFT) has been recently used [25-28] to describe the interaction between the inhibitor molecule and the surface as well as the properties of these inhibitors concerning their reactivity. For these seek, some molecular descriptors, such as HOMO and LUMO energy values, frontier orbital energy gap, molecular dipole moment, electronegativity ( $\chi$ ), global hardness ( $\eta$ ), softness (S), the fraction of electron transferred ( $\Delta N$ ), and molecular electrostatic potential (MEP) (MEP isoenergy surface maps were generated in the range from (deepest red color) to (deepest blue color), were calculated using the DFT method and have been used to understand the properties and activity of the newly prepared compounds and to help in the explanation of the experimental data obtained for the corrosion process.

According to Koopman's theorem [29] the ionization potential (IE) and electron affinity (EA) of the inhibitors are calculated using the following equations.

$$IE = -E_{\text{HOMO}}$$

$$EA = -E_{\text{LUMO}}$$

Thus, the values of the electronegativity ( $\chi$ ) and the chemical hardness ( $\eta$ ) according to Pearson, operational and approximate definitions can be evaluated using the following relations [30]:

$$\chi = \frac{IE + EA}{2}$$

$$\eta = \frac{IE - EA}{2}$$

Where the global softness is given by

$$S = \frac{1}{\eta}$$

The number of transferred electrons ( $\Delta N$ ) was also calculated depending on the quantum chemical method [31, 32] by using the equation;

$$\Delta N = \frac{\chi_{\text{Fe}} - \chi_{\text{inh}}}{2(\eta_{\text{Fe}^+} + \eta_{\text{inh}})}$$

Where  $\chi_{\text{Fe}}$  and  $\chi_{\text{inh}}$  denote the absolute electronegativity of iron and inhibitor molecule  $\eta_{\text{Fe}}$  and  $\eta_{\text{inh}}$  denote the absolute hardness of iron and the inhibitor molecule respectively. In this study, we use the theoretical value of  $\chi_{\text{Fe}} = 7.0 \text{ eV}$  and  $\eta_{\text{Fe}} = 0$ , for calculating the number of electron transferred.

Gaussian 03 [33] software package was used for theoretical calculation. The quantum chemical calculations were performed applying DFT method, with Beeke-3-Lee-Yang-Parr (B3LYP) supplemented with the standard 6-31G (d) basis set. All compounds have been optimized, where the ground state geometries and the frontier molecular orbital characteristics were analyzed on the optimized structures at the same level. In all cases, the steady state nature (minimum on the potential energy surface) of the optimized compounds has been confirmed by calculating the corresponding frequencies at the same computational level. The optimized geometry of the compounds under investigation in their ground states has been performed.

Since atomic charges has important role in many chemical reactions and for Physico chemical properties such as the molecular polarizability, dipole moment, electronic structure and more a lot of properties of molecular systems. Also, it affects the electrostatic interactions of the compounds. Thus, atomic charges are used for the description of the molecular polarity of molecules.

The total atomic charges of the four inhibitors under investigation are calculated using NBO [34] analysis as implemented in the Gaussian 03 program with B3LYP/6-31G(d) method and the results are Shown in Fig.5. Since, it is well known that the hetero atom with more negative charge is more reactive toward the interaction with the metal surface [35, 36]. Thus, from the resulted values one can conclude that that the two oxygen atoms of the two carbonyl groups as well as the three nitrogen atoms along with the two sulphur atom in the thiazole rings possess the highest negative atomic charges indicating that the compounds under investigation can effectively inhibit the corrosion of the steel through adsorption on its surface via their active sites (N and O and S atoms). The results of the quantum chemical calculations are depicted in Table 4.

HOMO and LUMO molecular orbital are calculated for all the Structures with B3LYP method using the 6-31Gd basis in the gas phase, giving rise to Fig.6. The eigen values of HOMO and LUMO and their energy gap reflects the chemical activity of the molecule. LUMO as an electron acceptor represents the ability to obtain an electron, whereas HOMO as an electron donor represents the ability to donate an electron.

**Table 4.** quantum chemical parameters for the different compounds as obtained from B3LYP/6-31G (d) method in the gas phase.

Comp.	$E_{\text{HOMO}}$	$E_{\text{LUMO}}$	$\Delta E_{\text{gap}}$	Dipole moment	$X(\text{ev})$	$\eta(\text{ev})$	$s(\text{ev})$	$\Delta N$
<i>o</i> -Bis-MeAT	-5.061	-0.890	4.171	3.508	2.976	2.087	0.479	0.965
<i>o</i> -Bis-AT	-5.207	-0.927	4.280	3.356	3.067	2.140	0.467	0.919
<i>p</i> -Bis-MeAT	-5.055	-0.503	4.551	4.528	2.779	2.276	0.439	0.928
<i>p</i> -Bis-AT	-5.168	-0.625	4.543	3.168	2.896	2.272	0.440	0.903

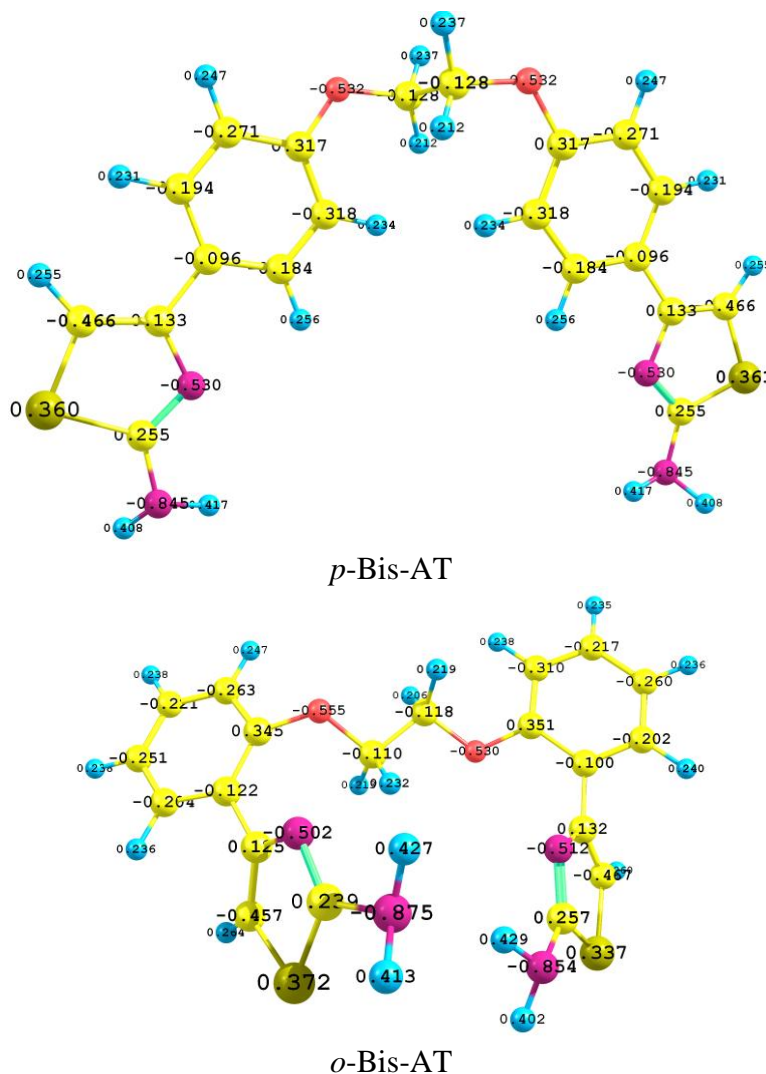


**Figure 5.** NBO atomic charges for the different inhibitors under investigation at B3LYP/6-31G (d).

The smaller, the energy gap of LUMO and HOMO, the easier, it is for the electrons of HOMO to be excited; the higher, the energies of HOMO, the easier, is for HOMO to donate electrons to the unoccupied d-orbital of the metal. In addition to that, the lower energy of LUMO, the easier, it is for LUMO to accepted electrons from metal surface. As the LUMO-HOMO energy gap decrease, the efficiency of inhibitor improved. The HOMO is delocalized on half molecule giving rise to two separated fragments in both compound *o*-Bis-MeAT and compound *o*-Bis-AT with high electron density concentrated on these fragments. This accounts for the higher ability of these inhibitors to chelate metal ions. In the other compounds *p*-Bis-MeAT and *p*-Bis-AT structures HOMO and LUMO are delocalized on the entire molecule, being the electronic density distributed all over the entire molecule.

The magnitudes of the energy gap of all compounds as obtained from the results of the quantum chemistry calculations depicted in Table 1, show that the compound *o*-Bis-MeAT and *o*-Bis-

MeAT possess the lowest energy gaps therefore, transfer of electrons from HOMO to LUMO is relatively easier thus expected to be more efficient corrosion inhibitor compared to the other compounds under investigation.

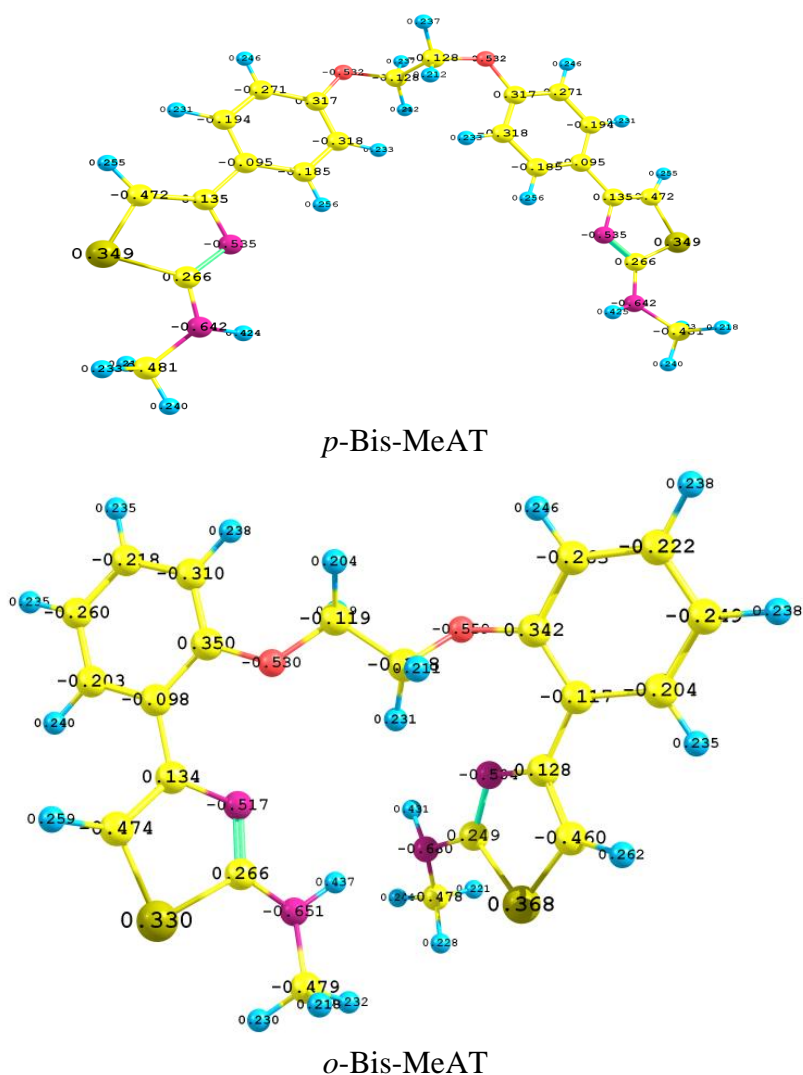


**Figure 5.** (continued)

Dipole moment (Table 4) shows the molecular charge distribution and is given as a vector in three dimensions. Therefore, it can be used as a descriptor to depict the charge movement across the molecule. Direction of the dipole moment vector in a molecule depends on the centers of positive and negative charges. The calculated dipole moment of the different inhibitors (Table 4) show the same trend as obtained for the energy gap between the HOMO and LUMO frontier molecular orbital. Some authors state that the inhibition efficiency increases with increasing value of the dipole moment depending on the compounds under investigation but in most cases no significant relationship has been found between the dipole moment values and the %IE. Besides, there is a lack of agreement in literature on the correlation between dipole moment and %IE [37, 38]. In this study we have obtained that the compound with the highest value of dipole moment shows a lower inhibition efficiency while

the compounds with lower values of dipole moment (Table 4) favors accumulation of the inhibitor on the surface layer and hence increases %IE.

Hardness is another molecular descriptor which is related to the activity of the compound. A hard molecule possesses a large gap between its HOMO and LUMO orbital and therefore less active which means low inhibition activity. Comparing the compounds under investigation shows the compound *o*-Bis-MeAT has the lowest value for hardness and compounds *p*-Bis-MeAT and *p*-Bis-AT shows the highest thus, they show the lowest inhibition.

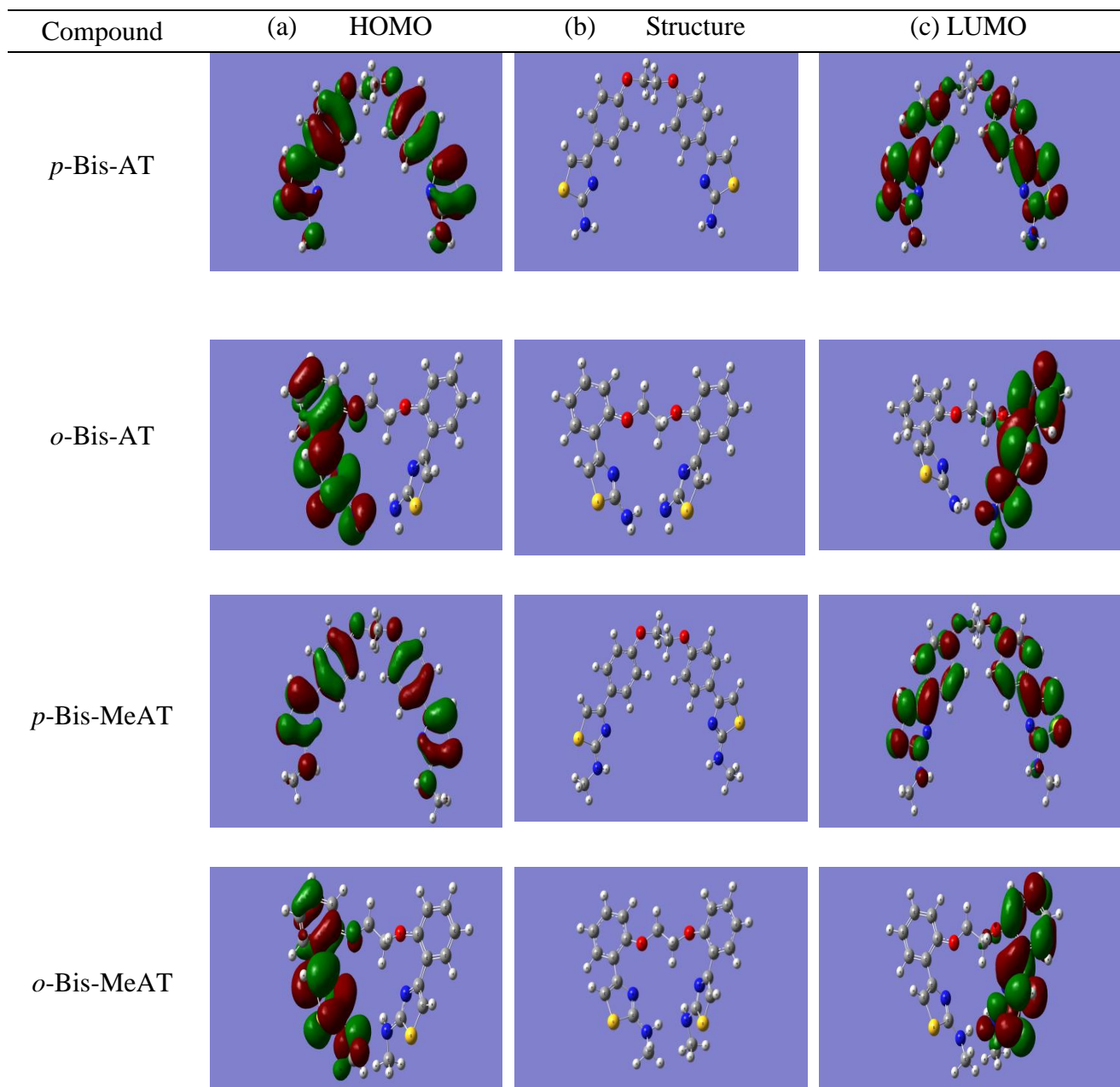


**Figure 6.** (a) HOMO plots of compounds at B3LYP/6-31G (d). (b) Optimized structures of the compounds at B3LYP/6-31G (d). (c) LUMO plots of compounds at B3LYP/6-31G (d).

Softness, which is the opposite of the hardness is showing an order of compound *o-Bis-MeAT* > *o-Bis-AT* > *p-Bis-AT* > *p-Bis-MeAT*, indicating that compounds *o-Bis-MeAT* and *o-Bis-AT* having the highest efficiency in inhibition.

The electron transfer between the inhibitor and the metal surface is an important descriptor used to determine the inhibition efficiency. Table 4 Shows that the values calculated for the amount of charge transferred for the compounds under investigation in this study shows the highest value of the electron transferred is 0.965 for compound *o-Bis-MeAT*, and hence show the highest inhibition efficiency. The order of the compounds according to the electron transferred was found to be Compound



Molecular electrostatic potential MEPs are calculated for all the optimized structures Fig.7. In all the structures the negative Charge density is localized on the oxygen atoms, and nitrogen atoms of the thiazole rings indicating a high ability in metal coordination.

In order to explore the dependence between the different molecular descriptors and the inhibition efficiency, correlation coefficient matrix has been obtained and the results are shown in Table 5. As may be seen, the inhibition efficiency (IE %) has good +ve correlation coefficients with softness(S) and the fraction of electron transferred ( $\Delta N$ ). It had correlation values 0.736314 and 0.804242 respectively. This means that as softness and the fraction of electron transfer increase, the inhibition efficiency increase. Whereas, the inhibition efficiency (IE%) has good -ve correlation coefficients with frontier orbital energy gap ( $\Delta E_{\text{gap}}$ ) and the global hardness ( $\eta$ ). It had a correlation values of -0.73868 and -0.73866 respectively. This means that as ( $\Delta E_{\text{gap}}$ ) and the fraction hardness ( $\eta$ ) increase, the inhibition efficiency decrease.

**Table 5.** Intercorrelation matrix for the parameters reported in Table 4.

	$E_{\text{HOMO}}$	$E_{\text{LUMO}}$	$\Delta E_{\text{gap}}$	Dipole moment	X(ev)	$\eta(\text{ev})$	s(ev)	$\Delta N$	IE%
$E_{\text{HOMO}}$	1								
$E_{\text{LUMO}}$	0.367694	1							
$\Delta E_{\text{gap}}$	-0.00619	0.927651	1						
Dipole moment	0.697311	0.61077	0.37585	1					
X(ev)	-0.62005	-0.95759	-0.78071	-0.7309	1				
$\eta(\text{ev})$	-0.00145	0.9294	0.999983	0.377019	-0.78365	1			
s(ev)	0.014359	-0.92453	-0.99991	-0.37641	0.77554	-0.99982	1		
$\Delta N$	0.692121	-0.41655	-0.72584	0.197525	0.136971	-0.7225	0.731573	1	
IE%	0.40834	-0.53372	-0.73868	0.332829	0.324148	-0.73866	0.736314	0.804242	1

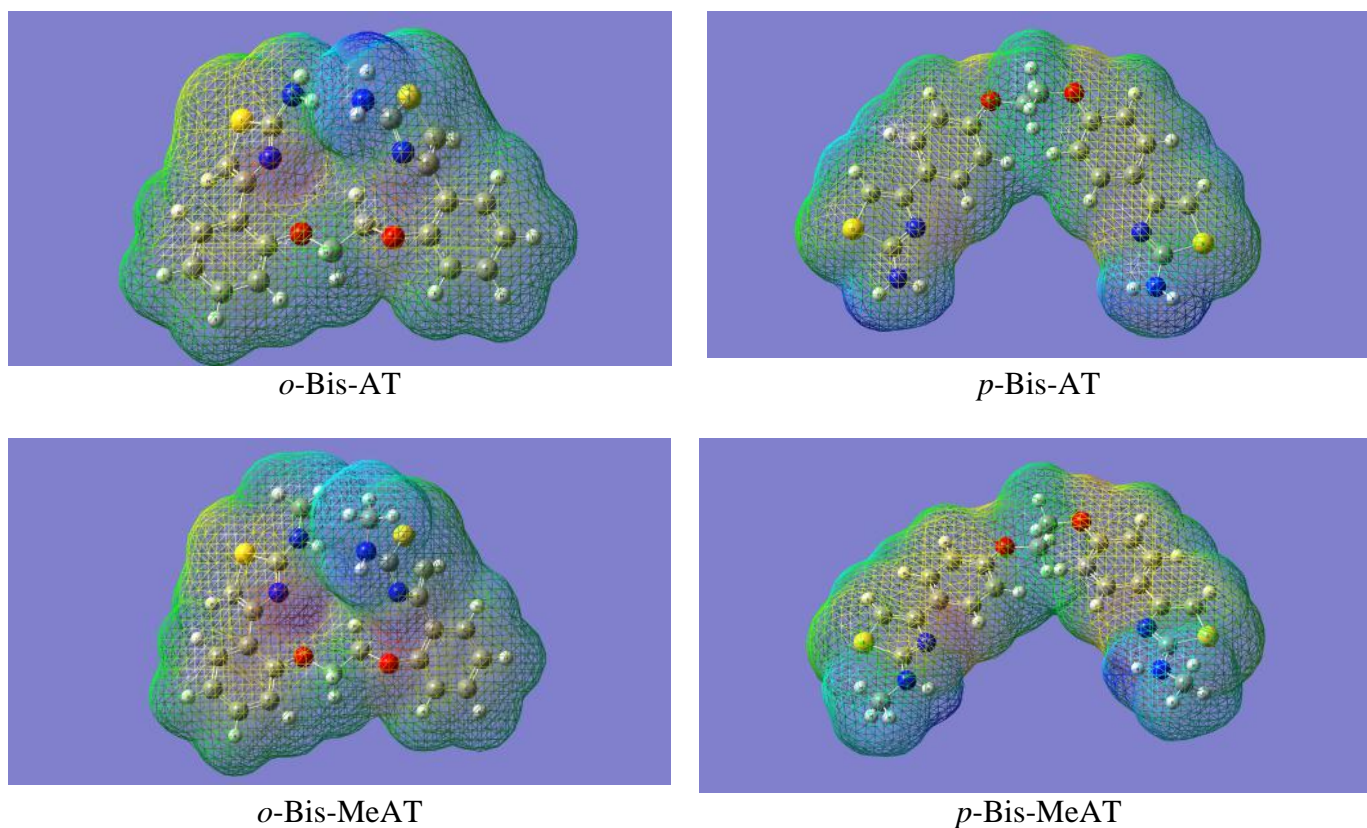


**Figure 7.** MESP of different compounds under investigation

## 5. INHIBITION MECHANISM

The corrosion of carbon steel in 0.5 M H<sub>2</sub>SO<sub>4</sub> solution and its inhibition by four compounds of novel derivatives was investigated using galvanostatic, potentiodynamic and weight loss techniques. The experimental data clearly demonstrate different inhibitor properties of the investigated compounds. It is interesting to find out which parameter of the molecular structure, electronic or the chemical structure (molecular surface area, position of the substituents, ect.) have major importance for the inhibitor efficiency.

The adsorption of bisaminothiazole molecules on the steel surfaces cannot be considered as purely physical or as purely chemical adsorption phenomenon. The spectrophotometric measurements showed that the adsorption of bis aminothiazole compounds on the carbon steel surface in 0.5 M H<sub>2</sub>SO<sub>4</sub> solution is more chemical adsorption than physical adsorption. Chemical adsorption of the investigated compounds arises from the donor acceptor interactions between free electron pairs of hetero atoms and  $\pi$ - electrons of multiple bonds as well as phenyl group and vacant d- orbitals of iron [39-41].

In order to confirm the possibility of the formation of Bis amino thiazole -Fe complex, UV-visible absorption spectra obtained from 0.5M H<sub>2</sub>SO<sub>4</sub> solution containing organic molecule before and after 3 days of carbon steel immersion are shown in Fig.8. Abboud et al. [42] has reported that change

in position of the absorbance maximum and change in the value of absorbance indicate the formation of a complex between two species in solution.

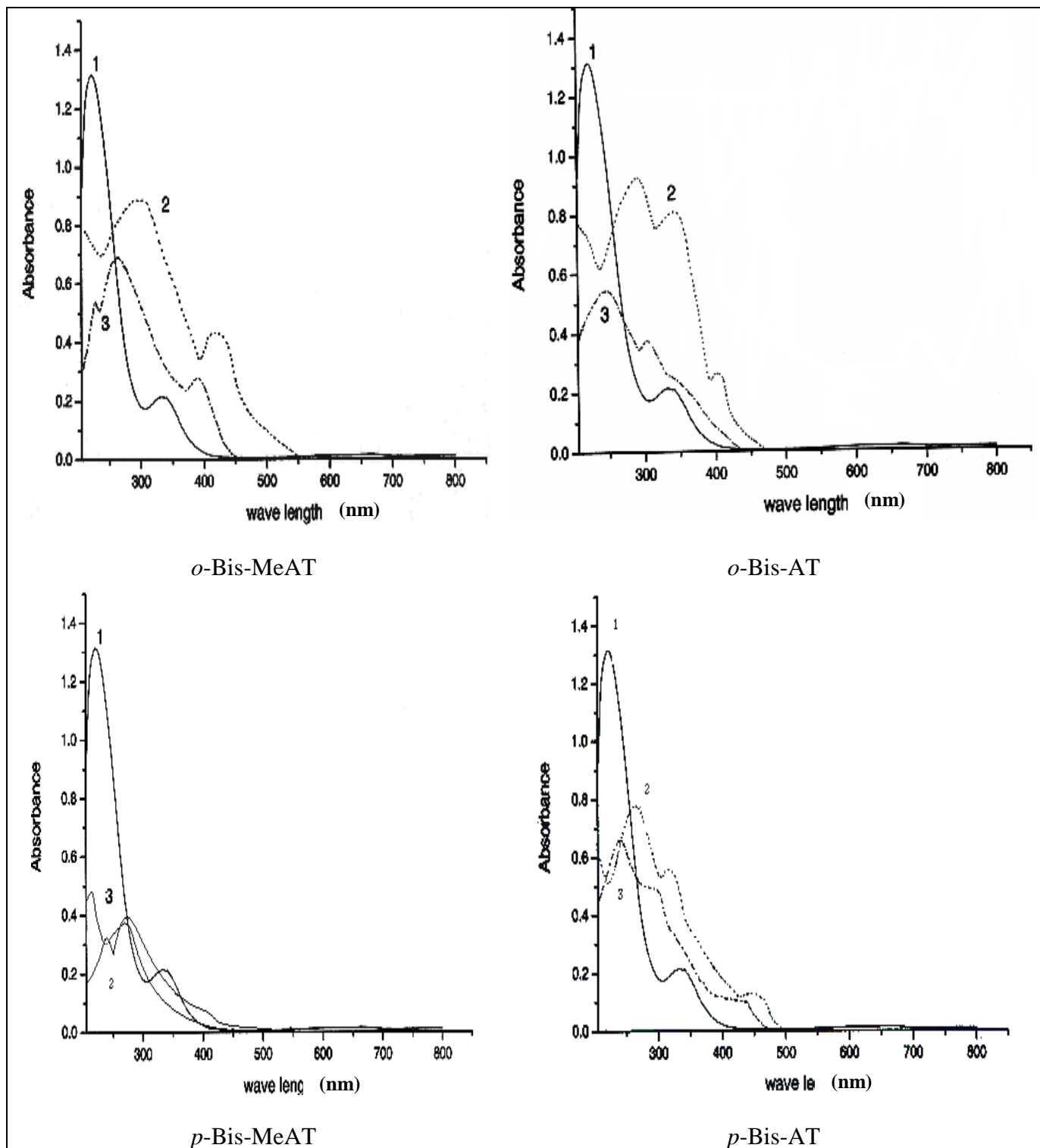
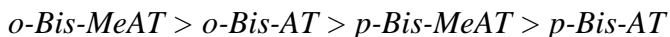


**Figure 8.** UV-spectra of the additive (4) used as inhibitor for carbon steel Corrosion in 0.5 M H<sub>2</sub>SO<sub>4</sub> solution (1) metal ion Fe<sup>+2</sup> (2) inhibitor molecule (3) mixture between them.

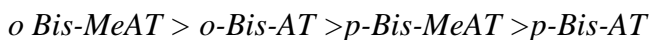
After 3 days of steel immersion (Fig.8), it is clearly seen that the band maximum underwent a blue shift. Furthermore, there is a change in the absorbance value of this band, suggesting the interaction between organic molecule and  $\text{Fe}^{+2}$  ions in the solution [43]. These experimental findings support the possibility of the complex formation between  $\text{Fe}^{+2}$  cation and bis amino thiazole molecule in 0.5M  $\text{H}_2\text{SO}_4$  solution.

The inhibition efficiency of bis amino thiazole compounds against the corrosion of carbon steel in 0.5M  $\text{H}_2\text{SO}_4$  follow the order:



at room temperature. The difference in the efficiency is referred to the molecular structure effect, to rigidity of  $\pi$ -delocalized system of the investigated molecules that may cause the increasing or decreasing of the electron density on center of adsorption, and leading to an easier electron transfer from the functional group to the metal, producing greater coordinate bonding and hence different adsorption and inhibition efficiency.

From the preceding discussion and in the light of data obtained from different techniques used. It is clearly found that the order of inhibition efficiency of bis amino thiazole compounds decreases in the following order:



It is worthy to mention that the o- bisaminothiazole compounds are more efficient than p-bisaminothiazole compounds. This efficiency was attributed to the ortho effect. o-Bis MeAT exhibits a good inhibition efficiency due to the presence of o- $\text{NHCH}_3$  which is an electro donating group leading to increase the electron charge density on the molecule and increase the surface coverage and facilitate the adsorption process. On the other hand o-BiAT compound is less inhibiting effect than o-Bis MeAT due the electro donation of  $\text{NH}_2$  group less than  $\text{NHCH}_3$  group. The same behavior occurred in para position.

## 6. CONCLUSIONS

Bisaminothiazole derivatives inhibit the corrosion of carbon steel in 0.5M  $\text{H}_2\text{SO}_4$  solution. The percentage inhibition efficiency was found to increase with increasing the concentration of inhibitors. The inhibitive effect was ascribed to the formation of insoluble complex adsorbed on the steel surface. The adsorption process follows Langmuir isotherm. Data obtained from quantum chemical calculations using DFT at the B3LYP/6-31G(d) level of theory were correlated to the inhibitive effect of bisaminothiazole compounds. Both experimental and theoretical calculations are in excellent agreement

## References

1. E.Sosa, R.Cabera-Sierra, M.T.Oropeza, *J. Appl. Electrochem.* 32 (2002) 905.
2. S.M.A.Hosseini, M.Salari, S.Jamalizadeh, S.Khezripoor, M.Seifi, *Mater. Chem. Phys.* 119 (2010) 100.

3. M. Abdallah, E.A. Helal, A.S. Fouda, *Corros. Sci.*, 48 (2006)1639.
4. M. Abdallah. *Mater. Chem. Phys.* 82(3), (2003) 786.
5. J. Cruz, R. Martinez, J. Genesca, E. Garcia-Ochoa., *J. of Electroanal. Chem.* 566 (2004) 111.
6. M. Abdallah, H.E. Megahed, M.Sobhi, *Mater. Chem. Phys.* 118 (2009)111.
7. M. Abdallah, H.E Megahed, M.Sobhi, *Monatsh. Chem.* 141 (2010) 1287.
8. M. Abdallah., I. Zaafarany, K.S. Khairou' M.Sobhi, *Int. J. Electrochem Sci.* 7(2) (2012)1564.
9. A.Chetouani,K.Medjahed,K.E.Sid-Lakhdar,B.Hammouti,M.Benkaddour A.Mansri, *Corros. Sci.* 46(2004)2421.
10. Xianghong Li, Shuduan Deng,Hui Fu, Taohong Li, *Electrochim.Acta.* 54 (2009)4089.
11. I.B.Obot N.O.Obi-Egbedi, *Corros. Sci.* 52(2010)657.
12. S.Issadi,T.Douadi,A.Zaouaoui,s.Chafaa,M.A.khan,G.Bouet,*Corros.Sci.* 53(2011)1484.
13. M.L. Zheludkevich ,K.A. Yasakau,S.K. Poznyak M.G.S. Ferreira, *Corros. Sci.*47 (2005) 3368.
14. Gy. Vastag, E. Szocs, A. Shaban, I. Bertoti, K. Popov-Pergal, E. Kalman, *Solid State Ionics* 141 (2001) 87.
15. O.K.Aboia, A.O. James, *Corros. Sci.* 52(2) (2010) 661.
16. N.O.Eddy, S.A.Odoemelam, *Pigment and Resin Technology* 38(2) (2009) 111.
17. A.J. Szyrowski, *Br. Corros. J.* 35(2)(2000)155.
18. S. L. Granese, B. M. Rosales, C. Oviedo, J. O. Zerbino, *Corros.Sci.* 33(1992)1439.
19. M. Abdallah, I. Zaafarany, J.H. Al-Fahemi, Y. Abdallah, A.S. Fouda, *Int.J.Electrochem Sci.* 7(8)(2012)6622.
20. A.S.Fouda, M. Abdallah, A.M. Atya, H.D. Sabaa, *Corrosion (NACE)* 68(7) (2012) 610.
21. K.F. Khaled, M.M. Al-Qahtani, *Mater. Chem. Phys.* 113(2009)150.
22. E. Stupnišek-Lisac, A. Gazivoda, M. Madzarac, *Electrochim. Acta* 47 (2002) 4189.
23. M.A. El-Morsi, *Corros. Sci.* 41(1999) 305.
24. M.Behpour, S.M.Ghoreishi, M. Khayatkashani, N. Soltani, *Mater. Chem. Phys.* 131(2012)621.
25. H.Ma,S.Chen,Z.Liu,Y.Sun, *J.Mol. Struct. (THEOCHEM)* 774 (2006) 1922.
26. J.H. Henrquez-Romn, L. Padilla-Campos, M.A. Pez, J.H. Zagal, M.A.Rubio, C.M.Rangel, J.Costamagna, G.Crdenas-Jirn, *J.Mol.Struct. (THEOCHEM)* 757 (2005)17.
27. L.M. Rodrigue-Valdez, A. Martnez-Villafane, D. Glossman-Mitnik, *J. Mol. Struct. (THEOCHEM)* 713 (2005) 6570.
28. Y.Feng, S.Chen, W.Guo, Y.Zhang, G.Liu, *J. Electroanal. Chem.* 602 (2007)115122.
29. M.J.S. Dewar, W. Thiel, *J. Am. Chem. Soc.* 99 (1977) 4899.
30. R.G. Pearson, *Inorg. Chem.* 27 (1988) 734.
31. V.S. Sastri, J.R. Perumareddi, *Corrosion(NACE)* 53 (1997) 617.
32. I. Lukovits, E. Kalman, F. Zucchi, *Corrosion(NACE)* 57 (2001)3.
33. M. J. Frisch, G. W. Trucks, H. B. Schlegel, G. E. Scuseria, M. A. Robb, J. R. Cheeseman, J. A. Montgomery, Jr., T. Vreven, K. N. Kudin, J. C. Burant, J. M. Millam, S. S. Iyengar, J. Tomasi, V. Barone, B. Mennucci, M. Cossi, G. Scalmani, N. Rega, G. A. Petersson, H. Nakatsuji, M. Hada, M. Ehara, K. Toyota, R. Fukuda, J. Hasegawa, M. Ishida, T. Nakajima, Y. Honda, O. Kitao, H. Nakai, M. Klene, X. Li, J. E. Knox, H. P. Hratchian, J. B. Cross, V. Bakken, C. Adamo, J. Jaramillo, R. Gomperts, R. E. Stratmann, O. Yazyev, A. J. Austin, R. Cammi, C. Pomelli, J. W. Ochterski, P. Y. Ayala, K. Morokuma, G. A. Voth, P. Salvador, J. J. Dannenberg, V. G. Zakrzewski, S. Dapprich, A. D. Daniels, M. C. Strain, O. Farkas, D. K. Malick, A. D. Rabuck, K. Raghavachari, J. B. Foresman, J. V. Ortiz, Q. Cui, A. G. Baboul, S. Clifford, J. Cioslowski, B. B. Stefanov, G. Liu, A. Liashenko, P. Piskorz, I. Komaromi, R. L. Martin, D. J. Fox, T. Keith, M. A. Al-Laham, C. Y. Peng, A. Nanayakkara, M. Challacombe, P. M. W. Gill, B. Johnson, W. Chen, M. W. Wong, C. Gonzalez, and J. A. Pople, *Gaussian 03, Revision E.01, Gaussian, Inc., Wallingford CT, 2004.*
34. F. Weinhold, C. Landis, Valency and Bonding, A Natural Bond Orbital Donor Acceptor Perspective; Cambridge University Press: Cambridge, U.K., 2005.
35. Bereket,G.;Ogretir,C.;Yurt,A. *J. Mol. Struct. (THEOCHEM)* 571(2001)139.

36. Bereket,G.;Hur,E.;Ogretir,C. . *J.Mol. Struct. (THEOCHEM)* 578 (2002) 79.
37. N .Khalil,. *Electrochim Acta* 48 (2003) 2635.
38. L.Rodriguez-Valdez, A.Martinez-Villafane, , D.Glossman Mitnik, *J. Mol. Struct. (THEOCHEM)* 713(2005) 65.
39. S. Kertit, B. Hammouti, *Appl. Surf. Sci.* 93(1996) 59.
40. M. Behpour, S.M. Ghoreishi, M. Salavati-Niasari, B. Ebrahimi, *Mater. Chem. Phys.* 107(2008)153.
41. I. Ahamad, M. A. Quraishi, *Corros. Sci.* 51(2009) 2006.
42. Y. Abboud, A. Abourriche, T. Saffaj, M. Berrada, M. Charrouf, A. Bennamara, H. Hannache, *Desalination*, 237 (2009) 175.
43. Y. Abboud, A. Abourriche, T. saffaj, M. Berrada, M. Charrouf, A. Bennamara, N. Al-Himidi, H. Hannache, *Mater. Chem. Phys.* 105(1) (2007) 1.

© 2014 The Authors. Published by ESG ([www.electrochemsci.org](http://www.electrochemsci.org)). This article is an open access article distributed under the terms and conditions of the Creative Commons Attribution license (<http://creativecommons.org/licenses/by/4.0/>).